JOURNAL OF CATALYSIS 105, 416–431 (1987)

Acidity and Catalytic Properties of H · Na-ZSM-8 Zeolite: Effect of H^+ Exchange, Pretreatment Condition, and Poisoning of Stronger Acid Sites

DEEPAK B. AKOLEKAR AND VASANT R. CHOUDHARY[1]

Chemical Engineering Division, National Chemical Laboratory, Pune 411 008, India

Received May 14, 1986; revised January 12, 1987

The influence of degree of H^+ exchange and calcination temperature of H · Na-ZSM-8 on its acidity distribution (measured by the chemisorption and stepwise thermal desorption of pyridine at 373–773 K) and catalytic properties for hydrocarbon conversion (viz., isomerization of *o*- and *m*-xylene and disproportionation of toluene) and methanol-to-aromatics conversion reactions have been investigated. Both the acidity and catalytic activity in these reactions increase with the decrease in Na^+ content and calcination temperature of the zeolite. The effect of poisoning of stronger acid sites with pyridine on the catalytic properties of the zeolite has also been studied. The catalytic activity and selectivity of the zeolite are strongly affected by this poisoning. The hydrocarbon conversion and aromatization reactions occur on strong protonic acid sites of the zeolite. Good correlations between catalytic activity and acidity (measured in terms of the chemisorption of pyridine at 673 K) have been obtained for these reactions. The increase in Na^+ content and calcination temperature and the poisoning have resulted in the increase in the shape selectivity of the zeolite in the formation of xylene isomers (i.e., the formation of *p*-xylene is increasingly favored) because of diffusion–reaction interactions. The physical, acidic, and catalytic properties, shape-selectivity behavior, and catalyst deactivation characteristics of ZSM-8 and ZSM-5 zeolites are compared.

INTRODUCTION

Since the introduction of ZSM-5 zeolite (*1*) by Mobil Oil Corporation in 1972, extensive studies have been reported, and this zeolite has gained increasing importance as a high-potential catalyst in a number of commercially important chemical processes (*2*). ZSM-8 zeolite (*3*) was introduced almost at the same time; however, only a few patents (*3–5*) on the synthesis and application of ZSM-8 as a catalyst have been reported so far. Levinbuk *et al.* (*6*) have reported the adsorption capacity of ZSM-8 for water, ammonia, and aliphatic hydrocarbons. Recently, Park and Chou (*7*) reported selective formation of alkyl aromatics in the alkylation of toluene with ethanol on ZSM-8. Chou *et al.* (*8*) observed that the molecular shape-selective characteristics of ZSM-8 and ZSM-5 zeolites are quite similar.

It is interesting that the X-ray powder diffraction spectra for ZSM-5 and ZSM-8 zeolites are somewhat similar; the difference lies mostly in the group reflections in the region $2\theta = 22–25°$; ZSM-8 shows a splitting in the highest peak which is not observed for ZSM-5 (*1, 3*). It is not yet clear whether the structure of ZSM-8 is significantly different from that of ZSM-5 or both these zeolites have a somewhat similar structures (*9*). Nevertheless, it is interesting to know the acid strength distribution and catalytic properties of ZSM-8 zeolite and the factors affecting these properties. Our earlier studies on H · Na-ZSM-5 zeolite (*10–12*) showed a strong influence of the degree of H^+ exchange and pretreatment condition on the acidic and catalytic properties of the zeolite. The present investigation was undertaken with the

[1] To whom all correspondence should be addressed.

0021-9517/87 $3.00

objective of studying the effect of the degree of cation exchange and calcination temperature of H · Na-ZSM-8 zeolite on its acid strength distribution (measured at temperatures close to that employed in catalytic processes by chemisorption and stepwise thermal desorption of pyridine) and catalytic activity and selectivity in methanol-to-aromatics and hydrocarbon conversion processes and also of studying the effect of selective poisoning of stronger acid sites of the zeolite on its catalytic properties.

EXPERIMENTAL

H · Na-ZSM-8 zeolites. Tetraethyl ammonium (TEA)-ZSM-8 (Si/Al = 29.6) zeolite was synthesized by hydrothermally treating a gel of composition 5.5 TEABr · $15.8Na_2O$ · $48.4SiO_2$ · $1.0Al_2O_3$ · $2054H_2O$ in a stirred stainless-steel autoclave (capacity 20 dm^3, stirring speed 70 rpm) at 453 K for 40 h at autogenous pressure (about 1250 kPa). The gel was prepared in the stirred autoclave by mixing thoroughly an alkaline solution of 4 kg of sodium silicate (containing Na_2O, 9.57%; SiO_2, 28.43%; and H_2O, 62.0%) and 0.45 kg of TEABr in 6 dm^3 of deionized water with an acidic solution of aluminum sulfate (prepared by dissolving 0.13 kg of anhydrous aluminum sulfate and 0.7 kg of concentrated sulfuric acid in 6 dm^3 of deionized water). After the hydrothermal synthesis, the contents of the autoclave were cooled to room temperature. The crystals of zeolite were filtered, washed thoroughly with deionized water, and dried in an air oven at 393 K for 24 h.

The organic part of the TEA · Na-ZSM-8 was removed by heating the zeolite in air at 813 K for 12 h (the temperature was increased at a heating rate of 10 K min^{-1}).

The zeolite with different degrees of H^+ exchange was prepared by repeatedly exchanging the calcined zeolite with 0.1 *M* HCl at 353 K. After H^+ exchange, the zeolite was washed with deionized water, dried in air at 393 K for 12 h, pressed without any binder, crushed to particles of 0.2–0.3 mm, and finally calcined in air at 813 K for 12 h (the temperature was raised at a heating rate of 10 K min^{-1}).

The degree of H^+ exchange (α) was determined by analyzing the Al and Na contents of the zeolite [α = (Al − Na)/Al].

The crystalline nature of the zeolite was determined by X-ray powder diffraction using a Holland Philips PW 1730 X-ray generator with a Ni-filtered Cu$K\alpha$ radiation source and a scintillation counter. The size and morphology of the crystals of the zeolite were studied with a Cambridge Stereoscan Model 150 scanning electron microscope. The zeolites (in fluorolobe mull) were examined for their –OH stretching bands (range 3200–3800 cm^{-1}) using a Perkin–Elmer 599B infrared spectrometer. The surface composition of the zeolite calcined at different temperatures (813-1273K) was studied by XPS using a VG Scientific ESCA-3MK II electron spectrometer.

The crystal density of the H-ZSM-8 (α = 0.96) and H-ZSM-5 (Si/Al = 17.2 and α = 0.99) zeolites and their sorption capacity for *n*-hexane and *p*-xylene at 303 K were determined by the specific gravity bottle method described earlier (*13*). The sorption of nitrogen in the zeolites at −78 K (at a relative pressure of 0.3) was measured using a Quantasorb surface area analyser (Quantochrome Corp.) based on the dynamic adsorption/desorption technique.

Measurement of stepwise thermal desorption (STD) of pyridine. The chemisorption of pyridine on the zeolites at 673 K was measured by the GC pulse technique (*14*) based on temperature-programmed desorption under chromatographic conditions.

The STD of pyridine was carried out by desorbing the pyridine chemisorbed at 373 K on the zeolite in a flow of nitrogen from 373 to 773 K in four steps (each of 100 K). The temperature in each step was raised at a linear heating rate of 10 K min^{-1}. After the maximum temperature of the respective step was attained, it was maintained for a period of 1 h to desorb the reversibly

TABLE 1

X-Ray Diffraction Data on H · Na-ZSM-8 (Si/Al = 29.6, α = 0.96)

d (Å)	I/I_0(%)	d (Å)	I/I_0(%)	d (Å)	I/I_0(%)
11.18	59.9	5.69	11.6	4.00	9.2
10.00	42.6	5.56	14.1	3.85	100.0
9.70	15.9	5.36	5.3	3.82	70.0
9.00	6.8	5.12	4.9	3.75	39.0
7.42	6.3	5.01	9.2	3.71	51.0
7.06	5.0	4.60	8.1	3.64	33.2
6.70	8.5	4.45	3.5	3.59	5.6
6.36	13.4	4.35	11.6	3.48	7.7
6.04	2.0	4.25	15.5	3.4	12.7
5.98	16.9	4.07	4.9	3.35	14.9

adsorbed base on the zeolite at that temperature.

Details of the procedure for the STD experiments are given elsewhere (*11, 15*).

Throughout this paper, the chemisorption is considered as the amount of base retained by the presaturated zeolite after it was swept with pure nitrogen for a period of 1 h.

Measurement of catalytic activity. The catalytic activity of the zeolites in the isomerization of *o*- and *m*-xylene, the disproportionation of toluene, and the methanol-to-aromatics conversion was determined in a pulse microreactor (i.d. 4 mm) connected to a gas chromatograph, under the following conditions: for isomerization of xylenes—amount of catalyst 0.05 g, N_2 flow rate 200 cm^3 min^{-1}, total pressure 238 kPa, temperature 673 K, and pulse size 0.05 mmol; for disproportionation of toluene and methanol-to-aromatics conversion—amount of catalyst 0.05 g, N_2 flow rate 20 cm^3 min^{-1}, total pressure 120 kPa, temperature 673 K, pulse size 0.01 mmol (toluene) and 0.025 mmol (methanol). Before the activity was measured, the catalyst was heated at 673 K for 1 h in a flow of nitrogen.

The catalytic activity of a poisoned zeolite, whose stronger acid sites were selectively blocked by pyridine chemisorbed at 773 K, was also measured under the above-mentioned conditions.

The reaction products were analyzed on a column of Betone-34 (5%) and dinonyl phthalate (5%) on Chromosorb-W (3 mm × 9 m) (carrier N_2 flow rate 20 cm^3 min^{-1}); the column temperature was programmed from 323 to 423 K at a heating rate of 10 K min^{-1}, keeping the initial and final temperatures for 10 and 30 min, respectively.

The details of the microreactor and the procedures for measuring the catalytic activity and for the selective poisoning of the zeolite were given earlier (*10, 11*).

RESULTS

Characterization of Zeolites

X-ray diffraction (XRD) data on H · Na-ZSM-8 (α = 0.96) are given in Table 1. The XRD data for the zeolite are similar to those for ZSM-8 reported elsewhere (*16*).

No significant change in the XRD pattern of the zeolite was observed when its degree of H^+ exchange (α) was varied from 0.08 to 0.96 and also when the calcination temperature of H · Na-ZSM-8 (α = 0.96) was increased from 813 to 1273 K, except that the intensity of peaks at lower angles ($2\theta < 18°$, i.e. $d > 5$ Å) was found to increase with the increase in calcination temperature, and for the zeolite calcined at 1273 K, the peak at $2\theta = 24.4°$ (i.e., $d = 3.64$ Å) was found to resolve into a doublet.

IR spectra of H · Na-ZSM-8 (α = 0.96) showed the –OH stretching band only at 3610 cm^{-1} and the intensity of this band was found to decrease with the increase in calcination temperature. The –OH band at 3720 cm^{-1}, which is expected for nonzeolite material (*17*), was found to be absent.

A scanning electron micrograph of the H · Na-ZSM-8 (α = 0.96) is shown in Fig. 1. The crystals of zeolite are cubical in shape and are nearly uniform in size (crystal size $\simeq$ 3.5 μm). The zeolite is also highly crystalline.

Physical properties of the ZSM-8 and ZSM-5 zeolites are compared in Table 2.

TABLE 2

Comparison of Physical Properties of H-ZSM-8 and H-ZSM-5 Zeolites

Zeolite	Si/Al ratio	α	Crystal size (μm)	Crystal density (g cm^{-3})	Sorption capacity (mmol g^{-1})		
					n-Hexane at 303 K	*p*-Xylene at 303 K	N_2 at −78 K (p/p_s = 0.3)
H-ZSM-8	29.6	0.96	3.5	1.75	1.33	1.13	4.9
H-ZSM-5	17.2	0.99	0.8	1.78	1.35	1.18	5.0

The results indicate that the two zeolites do not differ significantly in their crystal density and sorption capacity for *n*-hexane and *p*-xylene at 303 K and for nitrogen at −78 K.

XPS of the H · Na-ZSM-8 (α = 0.96) calcined at the different temperatures (813–1273 K) indicated that the concentration of aluminum on the surface of the zeolite crystals increased significantly with the increase in calcination temperature. This indicates the possibility of dealumination of the zeolite at higher temperatures (≥973 K), which is consistent with earlier observations on H-ZSM-5 zeolites (*10, 18*).

STD and Chemisorption of Pyridine

Figure 2 shows the results of the STD of pyridine from the H · Na-ZSM-8 zeolites. It may be noted that here the site energy is expressed in terms of a temperature range in which the base chemisorbed at the lowest temperature is desorbed (T_d is the desorption temperature of the base and T_d^* is the temperature at which the base chemisorbed on the strongest site is desorbed).

The temperature dependence of the chemisorption of pyridine on the zeolite with different degrees of H^+ exchange and the zeolite [H · Na-ZSM-8 with α = 0.96] calcined at different temperatures is shown in Fig. 3. The q_i (amount of pyridine chemisorbed) vs T (temperature) curves (Fig. 3) present a type of site energy distribution in which the number of sites are expressed in terms of the amount of pyridine chemisorbed as a function of chemisorption temperature, which, in turn, is a measure of

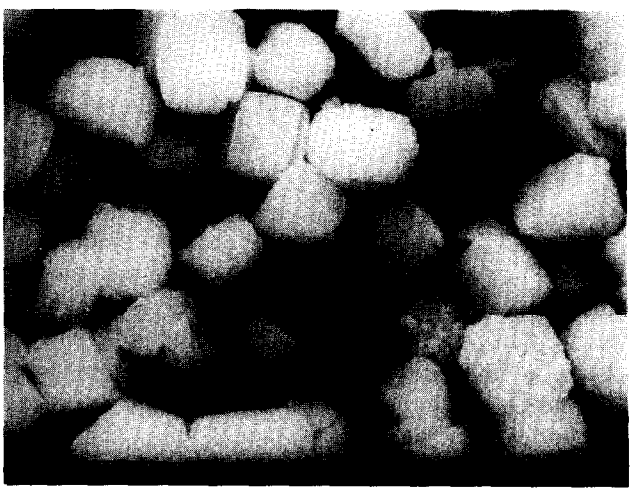

FIG. 1. Scanning electron microphotograph of H · Na-ZSM-8 (α = 0.96).

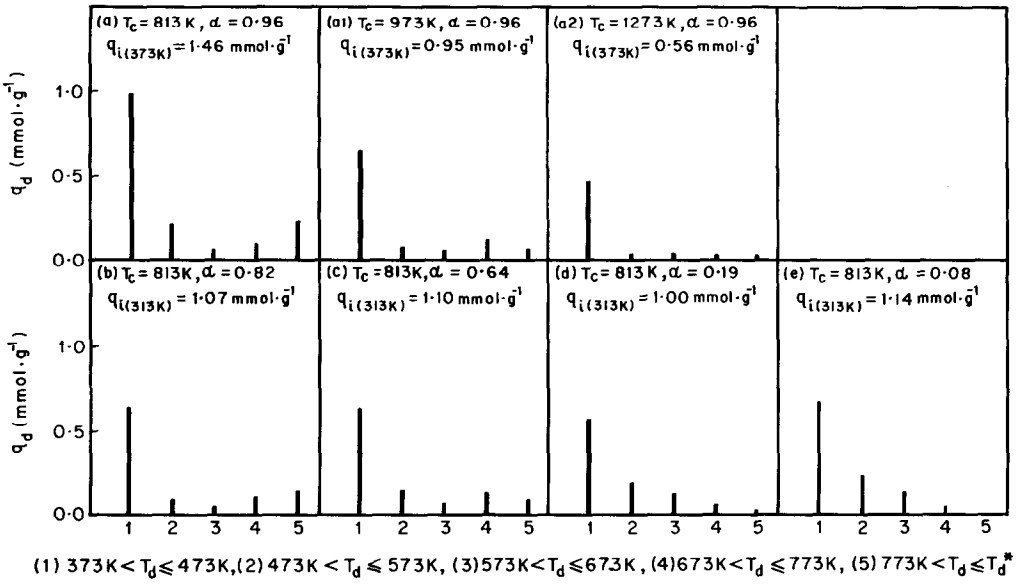

FIG. 2. Effect of calcination temperature (T_c) and degree of H^+ exchange (α) on the site energy distribution (obtained from the STD of pyridine) of H · Na-ZSM-8 zeolite.

the strength or energy of the sites involved in chemisorption. The results (Figs. 2 and 3) indicate that the site energy distribution and the number of strong sites (measured in terms of the chemisorption of pyridine at 673 K) on the zeolite are strongly influenced by its calcination temperature. The degree of cation exchange also affects the site energy distribution of the zeolite; however, its influence is strong, particularly, on high-energy (i.e., strong) sites. The number of strong sites on the zeolite increase with the increase in degree of H^+ exchange and decrease with the increase in calcination temperature. These observations are similar to those observed for ZSM-5 zeolite (*10–12*).

Catalytic Properties

The influence of the degree of H^+ exchange and the calcination temperature of the zeolite and of the poisoning of its stronger pyridine chemisorption sites on catalytic activity and product distribution (in the first pulse experiment) in *o*-xylene isomerization, toluene disproportionation, and methanol-to-aromatics conversion reactions has been shown in Figs. 4, 5, 6, and 7, respectively.

Effect of calcination temperature. The results (Figs. 4–7) show that the catalytic activity of the H · Na-ZSM-8 (α = 0.96) in the above reactions decreases almost exponentially with the increase in calcination temperature of the zeolite. The decrease in the catalytic activity is consistent with the decrease in the strong pyridine chemisorption sites of the zeolite.

In the *o*-xylene, toluene, and methanol conversion reactions, there is a very significant increase in the *p*-xylene/*m*-xylene (*p*-X/*m*-X) ratio with the increase in calcination temperature, thus showing an increase in the shape-selective behavior of the zeolite due to an increase in its calcination temperature. In the conversion of toluene, the benzene/xylene (B/X) ratio increases with the increase in calcination temperature of the zeolite.

It may be noted that the calcination temperature has no effect on the conversion of methanol to lower hydrocarbons; the con-

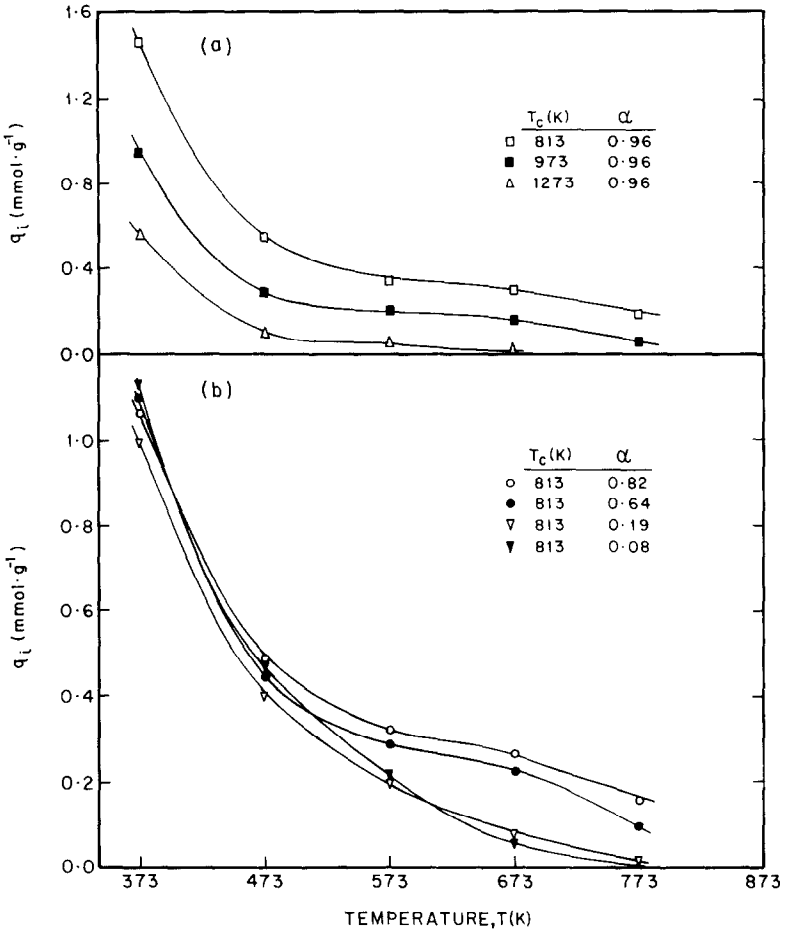

FIG. 3. Temperature dependence of chemisorption of pyridine (q_i) on H · Na-ZSM-8, showing the effect of calcination temperature (T_c) and degree of H^+ exchange (α).

version was nearly 100%. A similar observation was made for H-ZSM-5 zeolite (*11*). It is also interesting to note that the dependence of the catalytic activity and shape selectivity of H-ZSM-8 on calcination temperature is quite similar to that observed in the conversion of methanol and ethanol to aromatics on H · Na-ZSM-5 zeolite (*11*).

Effect of degree of H^+ exchange. The results show a strong influence of the degree of H^+ exchange on the catalytic activity and selectivity in the hydrocarbon and methanol conversion reactions (Figs. 4–7). The conversion of *o*-xylene, *m*-xylene, and toluene and the extent of aromatization in the methanol conversion increase with the increase in degree of H^+ exchange. The increase in catalytic activity in the above reactions is quite consistent with the increase in strong pyridine chemisorption sites on the zeolite. It can also be noted that the *p*-X/*m*-X ratio (in the conversions of *o*-xylene, toluene, and methanol) and the *p*-X/*o*-X ratio (in the methanol conversion) decrease with the increase in degree of H^+ exchange. In the methanol conversion on H · Na-ZSM-8 (α = 0.08), the *p*-X/*m*-X and *p*-X/*o*-X ratios have been found to be greater than 10. These facts indicate that the shape-selective behavior of the zeolite in the formation of xylene isomers decreases with

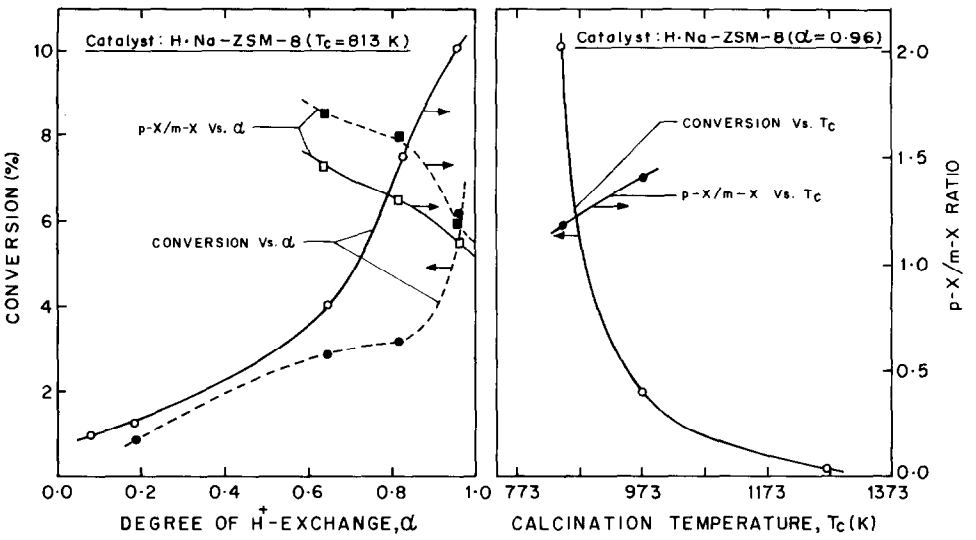

FIG. 4. Effect of degree of H^+ exchange (α), calcination temperature (T_c), and poisoning on conversion of *o*-xylene and *p*-X/*m*-X ratio in the isomerization of *o*-xylene on H · Na-ZSM-8 at 673 K [—, unpoisoned zeolite; ---, poisoned zeolite (by pyridine chemisorbed at 773 K)]. Amount of zeolite = 50 mg; N_2 flow rate = 200 cm^3 min^{-1}; pulse size = 6.0 μl.

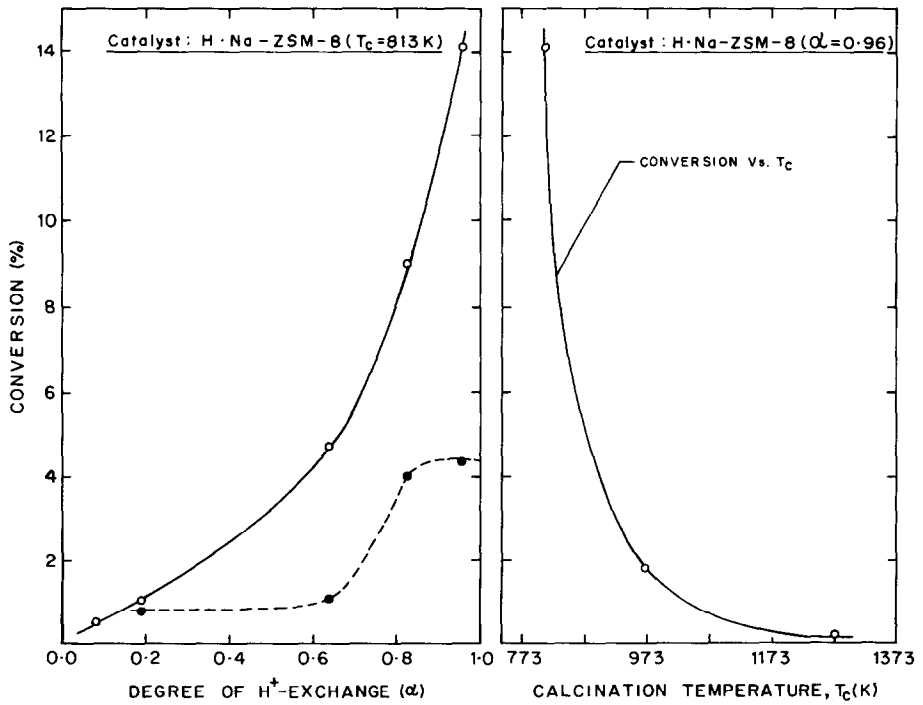

FIG. 5. Effect of degree of H^+ exchange (α), calcination temperature (T_c), and poisoning on conversion of *m*-xylene on H · Na-ZSM-8 at 673 K [—, unpoisoned zeolite; ---, poisoned zeolite (by pyridine chemisorbed at 773 K)]. Amount of zeolite = 50 mg; N_2 flow rate = 200 cm^3 min^{-1}; pulse size = 6.0 μl.

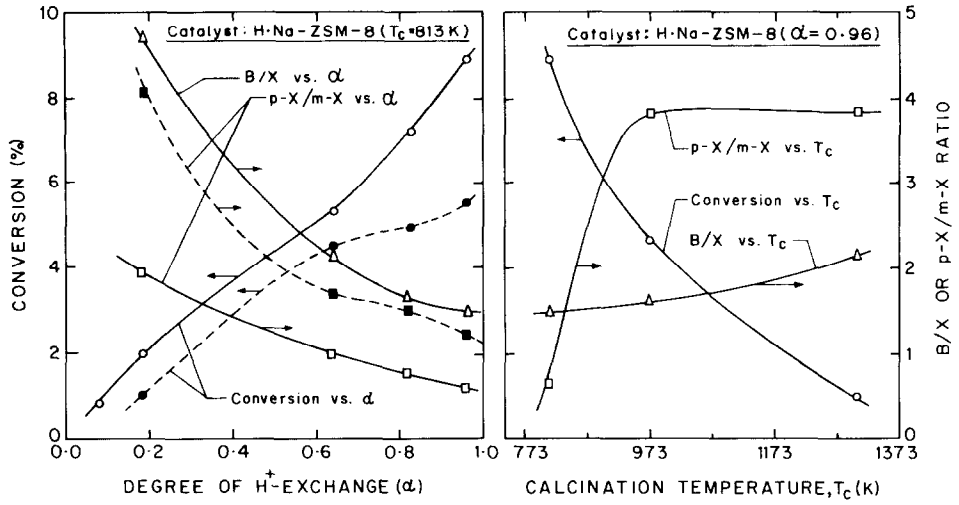

FIG. 6. Effect of degree of H^+ exchange (α), calcination temperature (T_c), and poisoning on conversion of toluene and B/X and *p*-X/*m*-X ratios in the disproportionation of toluene on H · Na-ZSM-8 at 673 K [—, unpoisoned zeolite; ---, poisoned zeolite (by pyridine chemisorbed at 773 K)]. Amount of zeolite = 50 mg; N_2 flow rate = 20 cm^3 min^{-1}; pulse size = 1.0 μl.

the increase in degree of H^+ exchange. It is also interesting to note that the B/X ratio in the conversion of toluene decreases with the increase in degree of H^+ exchange. This indicates that the disproportionation of toluene is favored over the dealkylation of

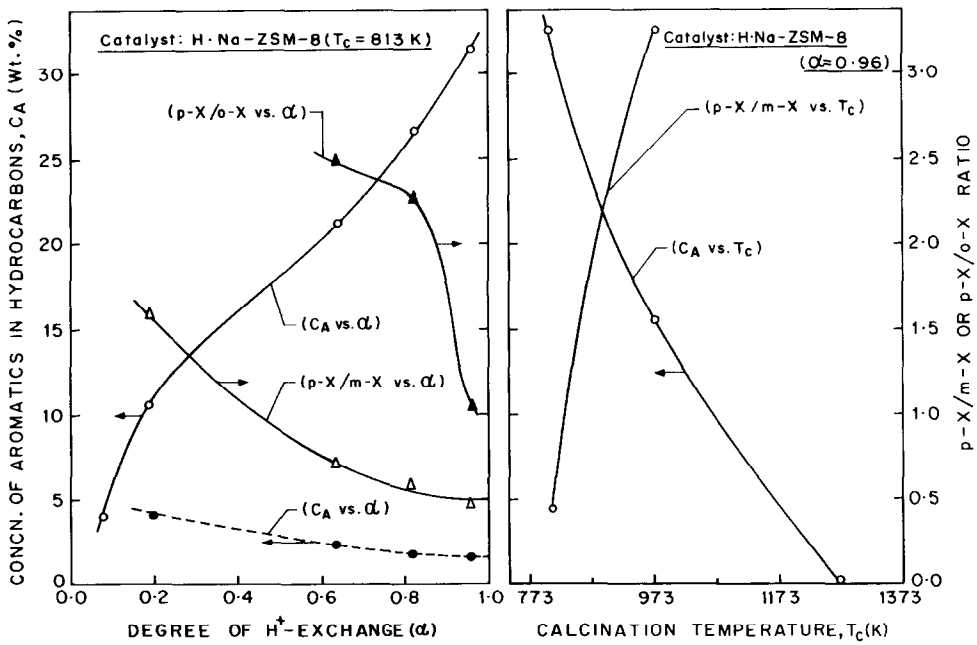

FIG. 7. Effect of degree of H^+ exchange (α), calcination temperature (T_c), and poisoning on aromatization and *p*-X/*m*-X and *p*-X/*o*-X ratios in the methanol-to-aromatics conversion on H · Na-ZSM-8 at 673 K [—, unpoisoned zeolite; ---, poisoned zeolite (by pyridine chemisorbed at 773 K)]. Amount of zeolite = 50 mg; N_2 flow rate = 20 cm^3 min^{-1}; pulse size = 1.0 μl.

toluene (occurring as a parallel reaction) on the zeolite having a higher degree of H^+ exchange.

The conversion of methanol to lower hydrocarbons on the zeolite with H^+-exchange values of 0.96, 0.82, and 0.64 was nearly 100%, but on the zeolite with H^+-exchange values of 0.19 and 0.08, conversion was 85.0 and 76.4%, respectively.

It may be noted that the effect of degree of H^+ exchange on the aromatization activity and shape-selectivity behavior of H · Na-ZSM-8 is quite similar to that observed in the conversion of methanol and ethanol to aromatics on H · Na-ZSM-5 zeolite (*19*).

Effect of poisoning. The poisoning of the zeolite by selective blockage of its stronger sites by the pyridine chemisorbed at 773 K caused a very significant decrease in the catalytic activity in all reactions (Figs. 4–7). This is a commonly observed poisoning effect. However, it is interesting that *p*-X/*m*-X ratio in the conversions of *o*-xylene, toluene, and methanol on the zeolite increases because of the poisoning. Thus, the poisoning results in an increase in the *para*-shape-selective behavior of the zeolite. Also interesting is that in the conversion of methanol, the aromatization activity of the poisoned zeolite decreases with the increase in degree of H^+ exchange.

It may be noted that the poisoning has not shown a significant effect on the conversion of methanol to lower hydrocarbons, which is similar to the observation made on H-ZSM-5 zeolite (*20, 21*). Also, the changes observed in the catalytic activity and shape-selectivity behavior of H-ZSM-8 due to the poisoning are quite similar to those observed for the H-ZSM-5 zeolite (*10, 20–22*).

Effect of pulse number. To compare the deactivation characteristics of ZSM-8 and ZSM-5 zeolites, a number of pulses of cumene were passed over the H-ZSM-8 (α = 0.96) and H-ZSM-5 (Si/Al = 17.2 and $\alpha >$ 0.99) zeolites one after the other at 1-h intervals at 600 K. The dependence of the cumene cracking activity [expressed in terms of the ratio of conversion of cumene in the *n*th pulse to that in the first pulse (x)] of the two zeolites on pulse number is shown in Fig. 8. A comparison of the results shows that the decrease in the cumene cracking activity of H-ZSM-8 with

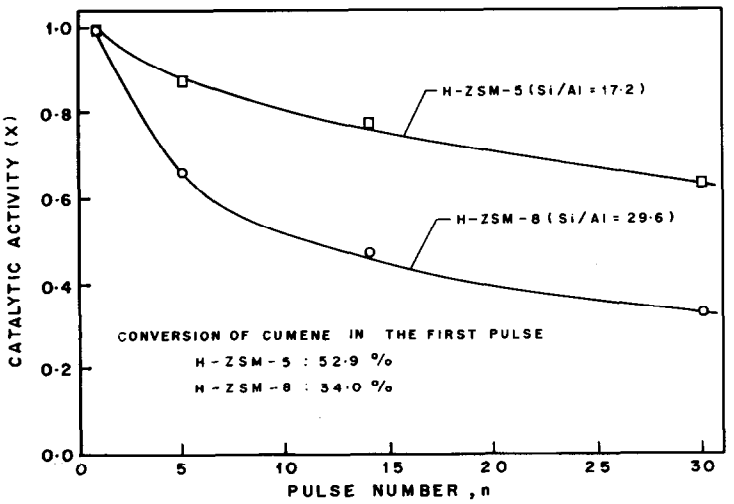

FIG. 8. Effect of pulse number on catalytic activity of the H-ZSM-8 and H-ZSM-5 zeolites in the cracking of cumene at 600 K. Amount of zeolite = 50 mg; N_2 flow rate = 1.0 dm^3 min^{-1}; pulse size = 8.0 μl.

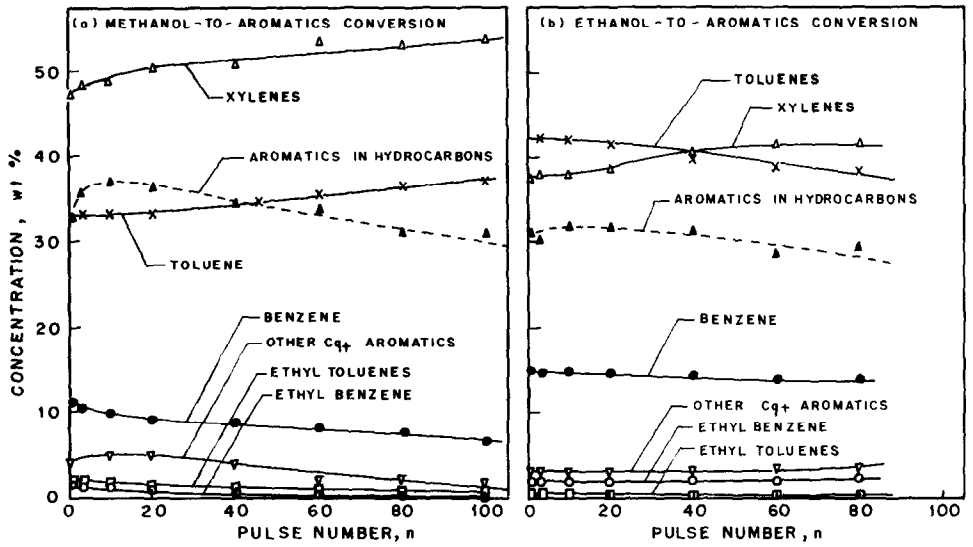

FIG. 9. Effect of pulse number on the aromatization activity and product distribution in the conversion of methanol and ethanol to aromatics on the H-ZSM-8 zeolite at 648 K. Amount of zeolite = 0.1 g; N_2 flow rate = 25 cm^3 min^{-1}; pulse size = 2.5 μl.

the increase in pulse number is much steeper than that for H-ZSM-5. When the partially deactivated H-ZSM-8 after the injection of 30th pulse was heated in a flow of nitrogen (100 cm^3 min^{-1}) at 773 K for 1 h, its cumene cracking activity (at 600 K) was found to increase from 0.33 to 0.8.

Figure 9 shows the effect of pulse number on aromatization activity and distribution of aromatics in the conversion of methanol and ethanol on H-ZSM-8 at 648 K. The results indicate that in both alcohol conversion reactions, the extent of aromatization increases to a small extent up to the injection of the 10th pulse, after which it decreases with increasing pulse number; the decrease is more significant in the methanol conversion. The relative distribution of aromatic hydrocarbons is also influenced significantly by the pulse number in both alcohol conversion reactions. However, the results of pulse experiments for the conversion of methanol (*21*) and ethanol (*23*) on H-ZSM-5 (Si/Al = 17.2) at 648 K (under conditions similar to those used for the alcohol conversions on H-ZSM-8 zeolite) showed that the extent of aromatization increases to a small extent up to injection of the 10th pulse (which is quite similar to that observed for the reactions on H-ZSM-8), after which it remains almost constant with increasing pulse number. Also, the distribution of aromatics in both alcohol conversion reactions was found not to be affected significantly by increasing pulse number. The initial increase in the aromatization with pulse number in the alcohol conversion reactions on both zeolites is expected to be due mostly to the gradual deactivation of very strong cracking sites.

DISCUSSION

Acidity Distribution

The chemisorption of pyridine on the zeolite (with different degrees of H^+ exchange) at 373–773 K (Fig. 3b) points to the fact that at lower temperatures, pyridine is not chemisorbed selectively only on acid sites; it can also interact strongly with nonacid sites, particularly with Na^+ cations at lower temperatures (*24*, *25*). Since the interaction between Na^+ and pyridine is

expected to increase with a decrease in the degree of H^+ exchange of the zeolite, the number of sites measured by the pyridine chemisorption at lower temperatures can be taken only as an upper limit of the acid sites in the zeolite. It may be noted that the effect of the degree of H^+ exchange on pyridine chemisorption becomes pronounced at higher temperatures. The number of sites measured by pyridine chemisorption increases as expected with the degree of H^+ exchange only above 623 K. At lower temperatures, the dependence is irregular (Fig. 3b). This is expected due to the weakening of the nonacid site–pyridine interactions at higher temperatures. Hence, for H · Na-ZSM-8 zeolites with a high degree of H^+ exchange (α = 0.82 and 0.96), the site energy distributions shown in Figs. 2 and 3 may be taken as equivalent to the acid strength distributions on the zeolites. But, for zeolites with a lower degree of H^+ exchange, only the data above 623 K are expected to represent the acidity distribution.

The dependence of strong acid sites of the zeolite, measured in terms of the pyridine chemisorbed at 673 K, on its degree of H^+ exchange and calcination temperature is presented in Fig. 10. The increase in acidity of the zeolite with the increase in degree of H^+ exchange is almost linear, whereas the decrease in acidity with increase in calcination temperature is exponential.

The decrease in the intensity of the –OH stretching band at 3610 cm^{-1} (which is expected to be responsible for protonic acid sites on the zeolites) and in the chemisorption of pyridine at 673 K with the increase in the calcination temperature of the zeolite indicated that the chemisorption of pyridine is essentially a measure of protonic acid sites in the H · Na-ZSM-8. The Lewis acid

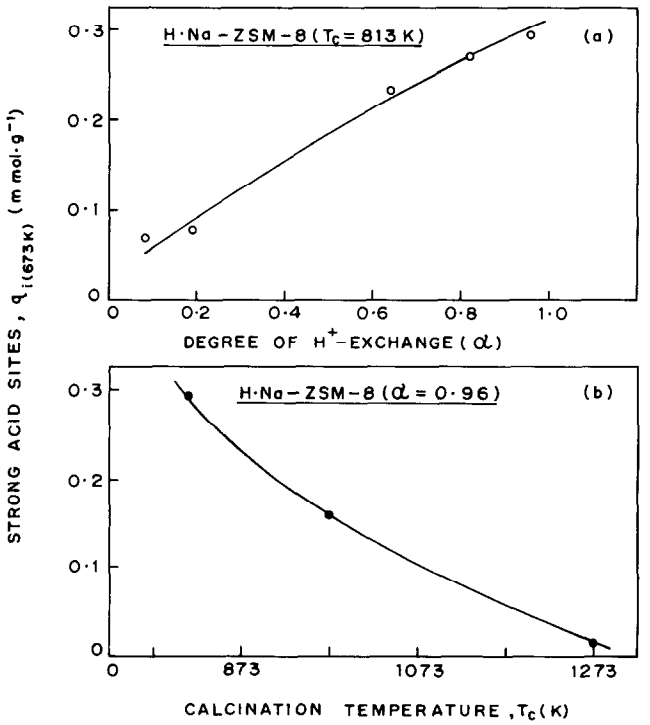

FIG. 10. Variation of strong acid sites on H · Na-ZSM-8 with its degree of H^+ exchange and calcination temperature.

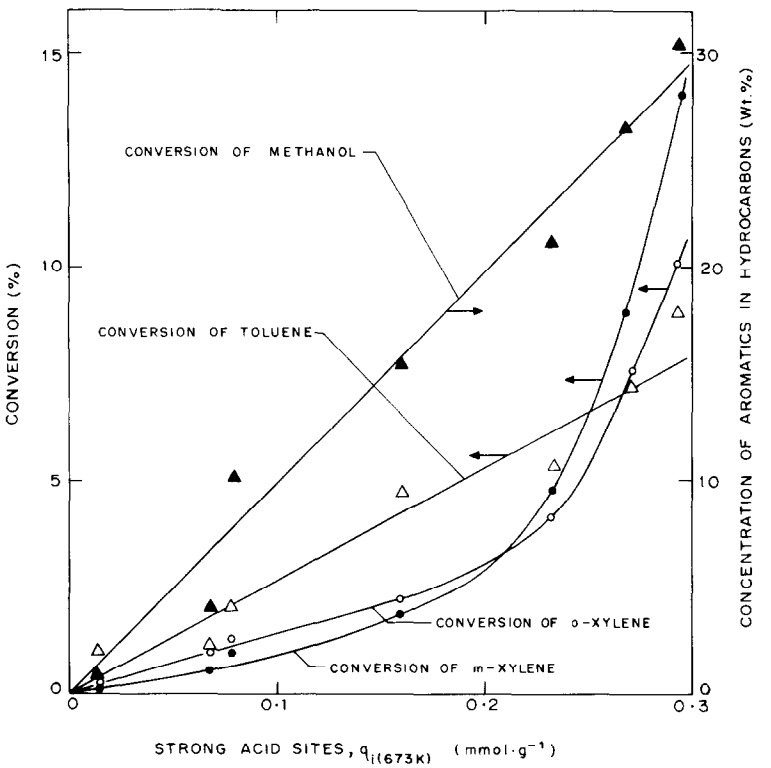

FIG. 11. Correlation between acidity and catalytic activity of H · Na-ZSM-8 in the conversions of *o*-xylene, *m*-xylene, toluene, and methanol.

sites formed due to dehydroxylation of the zeolite at higher calcination temperatures are not accessible to the base. This has also been observed in case of ZSM-5 zeolite (*11*).

The decrease in acidity (protonic) of the zeolite with the increase in calcination temperature is attributed mainly to the dehydroxylation at higher temperatures. To a small extent, this decrease in acid sites may also result from the dealumination of the zeolite observed at higher temperatures.

Correlation between Acidity and Catalytic Activity

In the hydrocarbon conversion (viz., isomerization of *o*-xylene and *m*-xylene and disproportionation of toluene) and methanol-to-aromatics conversion reactions on H · Na-ZSM-8, the catalytic activity depends strongly on the degree of H^+ exchange and calcination temperature. It may be noted that an increase in the degree of H^+ exchange and a decrease in the calcination temperature cause an increase in both the acidity (Fig. 10) and the catalytic activity (Figs. 4–7) of the zeolite in the above reactions. This fact indicates that the catalytic activity of the zeolite is related to its acidity. Correlations between the catalytic activity in different reactions and the acidity (strong acid sites measured in terms of the pyridine chemisorbed at 673 K) of H · Na-ZSM-8 are presented in Fig. 11.

The conversion of toluene and the extent of aromatization in the conversion of methanol increase almost linearly with the increase in acidity, indicating a linear relationship between the catalytic activity in these reactions and the acidity of the zeolite. The conversion of *o*-xylene or *m*-

xylene, however, increases exponentially with the increase in acidity. This apparent exponential increase in catalytic activity with acidity is expected mostly because of the intracrystalline mass transfer limitations imposed on the reaction by the higher critical size of *o*- or *m*-xylene molecules compared with methanol and toluene molecules (critical diameter: *o*-xylene, 0.74 nm; *m*-xylene, 0.74 nm; toluene, 0.67 nm; methanol, ≈0.44 nm).

The resistance to intracrystalline mass transfer of *o*- or *m*-xylene is expected to increase with the decrease in H^+ exchange (i.e., with the increase in Na^+ content) of the zeolite because of the larger size of Na^+ cation compared with the proton. Thus the higher content of Na^+ in the zeolite causes an increase in the diffusional resistance due to a small but significant decrease in the effective channel diameter of the zeolite. In earlier studies (*26*) on H · Na-ZSM-5 zeolite, a sharp increase in the diffusional resistance with the increase in Na^+ content was observed for the diffusion of benzene in the zeolite under catalytic conditions.

When the zeolite is calcined at higher temperatures, its protonic acidity is decreased due to dehydroxylation, but at the same time, dealumination to a small extent also occurs. The dehydroxylation and dealumination are also expected to cause a small but significant change in the effective channel diameter of the zeolite, which can significantly increase the diffusional resistance for xylene molecules because of their larger critical diameter.

For diffusion-controlled reaction (except for highly exothermic ones), the observed conversion is lower than that in the absence of mass transfer limitations. In the conversions of *o*-xylene and *m*-xylene on H · Na-ZSM-8, the increase in the mass transfer resistance with the increase in the Na^+ content and also the calcination temperature has thus resulted in an exponential increase in the observed catalytic activity with the increase in the acidity of the zeolite.

Active Acid Sites

The increase in the calcination temperature (which causes a decrease in the number of protonic acid sites by converting them into Lewis acid sites at higher temperatures) has resulted in a sharp decrease in the catalytic activity of the zeolite in all reactions (Figs. 4–7). This clearly points to the fact that the isomerization, disproportionation, and aromatization (in the methanol conversion) reactions on H · Na-ZSM-8 are catalyzed by protonic acid sites. Lewis acid sites are not involved in these reactions mostly because of their inaccessibility to the reacting molecules. It may be noted that the Lewis acid sites in H · Na-ZSM-8 are also not accessible to pyridine molecules (Fig. 10b) and therefore its chemisorption essentially measures the protonic acid sites in the channels of the zeolite.

It may be noted that the increase in the calcination temperature produces no significant effect on the conversion of methanol to lower hydrocarbons. This indicates that the Lewis acids formed at higher calcination temperatures are probably accessible to smaller molecules like methanol molecules.

The results of the selective poisoning of the stronger acid sites of the zeolite with pyridine (Figs. 4–7) show that the catalytic activity in the hydrocarbon conversion reactions and in the aromatization in the methanol conversion is reduced very significantly due to the poisoning. This indicates that the stronger acid sites are involved in these reactions. However, the poisoning showed no significant effect on the conversion of methanol to lower hydrocarbons, indicating that the dehydration of methanol occurs even on weaker acid sites.

It may be noted that the above observations are quite similar to those observed for H-ZSM-5 zeolite (*11, 19–22*).

It is interesting that the aromatization activity of the poisoned zeolite decreases with an increase in the degree of H^+

exchange (Fig. 7). This contradicts the results on unpoisoned zeolite and may be attributed to modification of the activity of the unpoisoned sites through their interactions with the chemisorbed pyridine and also to the distribution of the acid sites (which are not blocked by pyridine) on the poisoned zeolite. No firm conclusion on this matter can be drawn from this study.

Diffusion–Reaction Interaction Effects

The observed increase in the *p*-X/*m*-X ratio with the increase in Na^+ content and in the calcination temperature of the zeolite in the *o*-xylene isomerization, toluene disproportionation, and methanol-to-aromatics conversion reactions (Figs. 4–7) is a result of the diffusion–reaction interaction (*27*). The increase in diffusional resistance with the increase in Na^+ content of H · Na-ZSM-8 is expected because of the reduction in the effective channel diameter as H^+ (with negligibly small ionic diameter) is replaced by Na^+ (ionic diameter 0.19 nm) and also because of the stronger interaction of aromatic nuclei with Na^+ than with protons in the zeolite. The increase in diffusional resistance with the increase in calcination temperature is expected mostly because of the small but significant reduction in effective channel diameter resulting from the dehydroxylation and dealumination of the zeolite at higher temperatures. In the formation of xylene isomers in the above reactions, the selectivity for the *para* isomer increases with the increase in diffusional resistance in the zeolite, as the diffusivity of the *para* isomer is much higher than that of the other isomers; therefore, its formation is favored over that of other isomers because of the diffusion–reaction interaction. Similarly, the increase in the B/X ratio (in the toluene disproportionation) with the increase in Na^+ content of the zeolite (Fig. 6) is also due mostly to the increase in diffusional resistance in the zeolite. Aromatic hydrocarbons are expected to differ widely in their reactivities and diffusivities in a shape-selective zeolite like the present one. Also, the apparent reactivity is expected to increase with the decrease in diffusivity (*28*); hence, the formation of products possessing higher diffusivity is generally favored.

The results also show a strong influence of the poisoning of the zeolite on the *p*-X/*m*-X ratio in the *o*-xylene isomerization (Fig. 4) and toluene disproportionation (Fig. 6) reactions; the poisoning caused a marked increase in the *p*-X/*m*-X ratio. Also in this case, the increase in selectivity for the *para* isomer is expected mostly because of the increase in diffusional resistance in the zeolite resulting from the blockage of a fraction of a pathways in the volume or at the boundary of the zeolite crystal (*29*). A decrease in the diffusivity of the zeolite due to poisoning (or strongly presorbed polar compounds) is commonly observed (*30*). This has also been observed for ZSM-5 zeolites (*31, 32*).

It is interesting to note that the *para*-shape-selectivity behavior of the ZSM-8-type zeolites, discussed above, is quite similar to that observed for ZSM-5-type zeolites (*10, 11, 19–22*). This is consistent with earlier observation on ZSM-8-type zeolites. (*8*).

Catalyst Deactivation

The results in Figs. 8 and 9 indicate that the catalytic activity in cumene cracking and alcohol-to-aromatics conversions reactions on H-ZSM-8 zeolite decreases with the increase in pulse number. The fact that heating of the deactivated zeolite at elevated temperature (773 K) in an inert atmosphere results in a partial gain of its catalytic activity reveals that the catalyst deactivation occurs mostly because of blockage of zeolite channels by strongly adsorbed large hydrocarbon molecules, which are cracked to smaller fragments at higher temperature.

Comparison between ZSM-8 and ZSM-5 Zeolites

The crystal density and sorption capacity

for *n*-hexane, *p*-xylene, and nitrogen of H-ZSM-8 zeolite are quite close to those for H-ZSM-5 zeolite (Table 2), indicating that these two zeolites do not differ significantly in their physical properties.

The effects of calcination temperature and degree of H^+ exchange on the number of strong acid sites (measured in terms of pyridine chemisorbed at 673 K) of H · Na-ZSM-8 are quite similar to those observed for H · Na-ZSM-5 zeolite (*10–12*). It is, however, interesting that the number of strong acid sites on H-ZSM-8 is 0.29 mmol g^{-1}, which is somewhat higher than the number of strong acid sites (0.25 mmol g^{-1}) (*33*) on H-ZSM-5 having the same Si/Al ratio.

Comparison of the results on ZSM-8 type zeolite, showing the effect of calcination temperature, degree of H^+ exchange, and poisoning of strong acid sites by pyridine on catalytic activity and *para*-shape selectivity in hydrocarbon conversion and alcohol-to-aromatics conversion reactions, with the results on ZSM-5-type zeolites (*10, 11, 19–22*) clearly indicates a close similarity. The nature of active acid sites and their strength requirements for catalyzing the reactions for these two zeolites are also similar. However, though both zeolites possess almost similar shape-selective properties, ZSM-8-type zeolites undergo catalyst deactivation at a faster rate than do ZSM-5-type zeolites. This is expected because of the small but significant difference in channel structure between the two zeolites.

CONCLUSIONS

The following conclusions are drawn from studies on H · Na-ZSM-8 zeolite with respect to acidity and catalytic properties and factors affecting these properties.

The acidity and catalytic activity (in the conversions of *o*-xylene, *m*-xylene, and toluene and in the aromatization in the conversion of methanol) of H · Na-ZSM-8 are strongly influenced by the degree of H^+ exchange and the calcination temperature of the zeolite. Both the acidity and catalytic activity of the zeolite decrease with the increase in Na^+ content and calcination temperature. The catalytic activity of the zeolite in the above reactions is correlated with the acidity measured in terms of the pyridine chemisorbed at 673 K. The chemisorption of pyridine at higher temperatures (>623 K) essentially measures protonic acid sites on the zeolite.

The active acid sites on the zeolite for the hydrocarbon conversion and aromatization reactions are protonic, and these reactions occur on the strong protonic acid sites; however, the dehydration of methanol to lower hydrocarbons can occur even on weaker acid sites.

Both the catalytic activity and product selectivity in the above reactions are strongly affected by the poisoning of stronger acid sites of the zeolite by pyridine.

The shape selectivity of H · Na-ZSM-8 in the formation of xylene isomers in the hydrocarbon conversion and aromatization reactions increases (i.e., the formation of *p*-xylene is favored over other xylene isomers) with the increase in Na^+ content and calcination temperature of the zeolite; it also increases after poisoning of the zeolite, mostly because of the increase in the diffusional resistance in the zeolite, resulting in increased diffusion–reaction interactions leading to the formation of products having higher diffusivity.

Comparison of the results on ZSM-8-type zeolites with those observed on ZSM-5 type zeolites indicates a close similarity between these zeolites in their physical properties (viz., crystal density and sorption capacity), acidity, active sites, catalytic properties, and shape-selective behavior. However, the observed higher rates of catalyst deactivation due to the deposition of large hydrocarbon molecules in the channels of ZSM-8-type zeolites indicate the possibility of a small but significant difference in the channel structure of the two zeolites.

REFERENCES

1. Argauer, R. J., and Landolt, G. R., U.S. Patent 3,702,886 (1972).
2. Scott, J. (Ed.), "Zeolite Technology and Applications—Recent Advances," Noyes Data Corp., NJ, 1980.
3. Mobil Oil Corp., Netherlands Patent, 7,014,807 (1971).
4. Vybihal, J., Czechoslovakian CS 211,981 (Cl. CO18 33/28), 29 Jul 1983, Appl. 80/7,602,4 (1980).
5. Chen, N. Y., Lucki, S. J., and Garwood, W. E., U.S. Patent 3,700,585 (1972).
6. Levinbuk, M. I., Khadzhiev, S. N., Limova, T. V., Meged, N. F., Topchieva, K. V., and Mironova, L. P., *Vestn. Mosk. Univ. Ser. 2 Khim.* **20**(2), 177 (1979).
7. Park, S., and Chou, H., *Chem. Eng. Commun.* **34,** 137 (1985).
8. Chou, H., Ahn, B. J., and Park, S. E., "Proc. 8th Int. Congr. Catal., 1984," Vol. 4, IV 555, Verlag Chemie, Weinheim, 1985.
9. Lechert, H., *NATO ASI Ser, Ser. E* **80,** 151 (1984).
10. Nayak, V. S., and Choudhary, V. R., *Appl. Catal.* **4,** 333 (1982).
11. Nayak, V. S., and Choudhary, V. R., *J. Catal.* **81,** 26 (1983).
12. Nayak, V. S., and Choudhary, V. R., *Zeolites* **5,** 15 (1985).
13. Choudhary, V. R., and Singh, A. P., *Zeolites* **6,** 206 (1986).
14. Choudhary, V. R., and Nayak, V. S., *Appl. Catal.* **4,** 31 (1982).
15. Choudhary, V. R., *J. Chromatogr.* **268,** 207 (1983).
16. Breck, D. W., "Zeolite Molecular Sieves" (D. W. Breck, Ed.), p. 373. Wiley, New York, 1974.
17. Jacobs, P. A., and von Ballmoos, R., *J. Phys. Chem.* **86,** 3050 (1982).
18. Vedrine, J. C., Auroux, A., Bolis, V., Dejaifve, P., Naccache, C., Wierzchowshi, P., Derouane, E. G., Nagy, J. B., Gilson, J. P., van Hoof, J. H. C., van den Berg, J. P., and Wotthuizen, J., *J. Catal.* **59,** 248 (1979).
19. Choudhary, V. R., and Nayak, V. S., *Zeolites* **5,** 325 (1985).
20. Nayak, V. S., and Choudhary, V. R., *Appl. Catal.* **9,** 251 (1984).
21. Choudhary, V. R., and Sansare, S. D., *Indian J. Technol.* **23,** 326 (1985).
22. Choudhary, V. R., and Nayak, V. S., *Indian J. Technol.* **21,** 376 (1983).
23. Choudhary, V. R., and Sansare, S. D., *Appl. Catal.* **10,** 147 (1984).
24. Jacobs, P. A., *in* "Carbonigenic Activity of Zeolites." Elsevier, Amsterdam, 1977.
25. Choudhary, V. R., *J. Chromatogr.* **259,** 283 (1983).
26. Choudhary, V. R., and Srinivasan, K. R., *J. Catal.* **102,** 289 (1986).
27. Weisz, P. B., *Pure Appl. Chem.* **52,** 2091 (1980).
28. Anderson, J. R., Mole, T., and Christov, V., *J. Catal.* **61,** 477 (1980).
29. Theodorou, D., and Wei, J., *J. Catal.* **83,** 205 (1983).
30. Barrer, R. M., *Adv. Chem. Ser.* **102,** 1 (1971).
31. Nayak, V. S., and Riekert, L., "International Symposium on Zeolite Catalysis, May 13–16, 1985, Siofok (Hungary)," preprints, p. 157.
32. Choudhary, V. R., and Singh, A. P., unpublished work.
33. Choudhary, V. R., and Nayak, V. S., *Mat. Chem. Phys.* **11,** 515 (1984).